

Non-destructive study of non-equilibrium states of cold, trapped atoms

Maria Brzozowska, Tomasz M. Brzozowski, Jerzy Zachorowski, and Wojciech Gawlik*
Marian Smoluchowski Institute of Physics, Jagiellonian University, Reymonta 4, PL 30-059 Cracow[†]
 (Dated: 9th November 2018)

Highly sensitive, non-destructive, real-time spectroscopic determination of the 2D kinetic momentum distribution of a cold-atom sample is performed with the three-beam measurement of the recoil-induced resonances. The measurements performed with an operating magneto-optical trap reveal slow velocity drifts within a stationary atomic cloud and strong anisotropy and asymmetry of the non-Maxwellian momentum distribution. The developed method can be easily extended to 3D.

PACS numbers: 32.80.Pj, 42.50.Vk, 42.65.-k

Most experiments with cold, dilute atomic gases employ magneto-optical traps (MOT), which yield temperatures in a range of hundreds to a few μK . Further traps and cooling stages can be applied for reaching the quantum degeneracy regime. This requires matching of the momentum distributions of various traps. Knowledge of such distributions is also essential for quantum state diagnostics of the trapped sample. Below, we present reliable method of 2D momentum diagnostics based on the so called recoil-induced resonances (RIRs) and apply it to the detailed study of non-standard momentum distributions in a MOT.

The first unambiguous observation of RIRs was made in a 1D optical lattice [1] filled with atoms much colder than in a standard MOT. RIR signals were also seen in optical molasses [2, 3], in a cold atomic beam [4] and with atoms released from a MOT [5]. The influence of the recoil effect on the probe absorption and four wave mixing spectra has been recently demonstrated in a continuously working MOT, i.e. with all light and magnetic fields on, in [6].

In this Letter we present evidence of three different kinds of anisotropy of the momentum distribution in an operating MOT. The measurements were conducted using our three-beam, RIR-based method developed for simultaneous probing of the momentum distribution in two perpendicular directions. The method extends the principle of 1D thermometry as suggested in Ref. [2]. Important feature of our extension is that 2D information is acquired simultaneously in one measurement. The method can be extended to 3D.

The RIRs result from a stimulated Raman process, which couples two kinetic states of free moving atoms (Fig. 1). Two laser beams, the pump and the probe, of frequencies ω and $\omega + \delta$, respectively, drive the Raman transition after which the atoms gain kinetic energy $\Delta E_{\text{kin}} = \hbar\delta$ and change momentum \mathbf{p} by $\Delta\mathbf{p} = \hbar\Delta\mathbf{k} = \pm 2\hbar k\hat{\mathbf{e}}_i \sin\theta/2$, where k is the modulus of the light wave vector, θ is the angle between the beams,

and $\hat{\mathbf{e}}_i$ is the unit vector perpendicular to the bisector of θ . The non-zero amplitude of the considered Raman resonance arises from different populations of the given kinetic states. When recorded in absorption, the RIR shape is proportional to a derivative of the momentum distribution $\partial\Pi(p_i)/\partial p_i$, where $p_i = \mathbf{p} \cdot \hat{\mathbf{e}}_i$ [1, 6, 7, 8]. This direct relation of the RIR signal to $\Pi(\mathbf{p})$ allows convenient and accurate measurement of the kinetic momentum distribution in a cold atomic sample, provided that the distribution is sufficiently narrow.

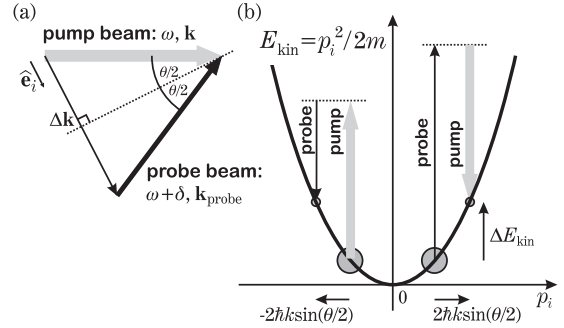


Figure 1: Recoil-induced resonances: (a) geometry of the laser beams, (b) atomic kinetic energy and momentum changes due to the Raman process coupling two kinetic states. Circles symbolize populations $\Pi(\mathbf{p})$ of these states.

Important advantage of the RIR method is its directional selectivity. $\Pi(\mathbf{p})$ is probed in a given direction, specified by $\Delta\mathbf{p}$, i.e. by angle θ (Fig.1a). Hence, apart from applications to standard 1D velocimetry [2, 4], RIRs can also be used for studies of a possible momentum distribution anisotropy in non-equilibrium states of a cold atomic sample.

Our experiment (Fig. 2) employs a standard vapor-loaded MOT [9] with ^{85}Rb atoms. Two extra beams intersect in the trap center: the pump and the probe. The probe beam is directed at a small angle $\alpha = 3^\circ$ to the MOT beams (propagating along z), and the pump is at $\theta = 5^\circ$ to the probe. The probe beam can be detected either directly or after retroreflection. The setup with retroreflected probe enables the measurement of $\Pi(\mathbf{p})$ simultaneously along two perpendicular directions: \perp , for angle θ between the pump and the nearly co-propagating

*Electronic address: gawlik@uj.edu.pl

[†]URL: <http://www.if.uj.edu.pl/ZF/qnog/>

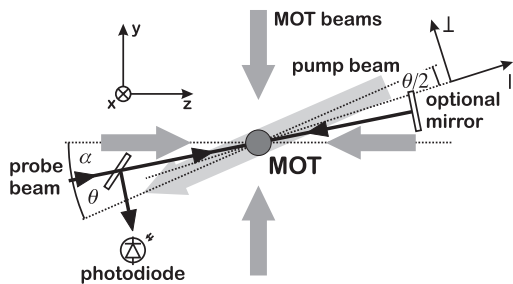


Figure 2: The layout of the experiment. The pump and probe beams intersect in a cloud of cold atoms. With the optional mirror we realize a three-beam configuration in which the momentum exchange is allowed in two directions: \perp and \parallel . Third pair of the MOT beams along x and the MOT coils are not shown in this figure.

probe, and \parallel , for angle $180^\circ - \theta$ between the pump and the nearly counter-propagating probe. When α and θ are sufficiently small, \perp and \parallel almost coincide with the y and z directions, respectively. Both pump and probe beams are derived from diode lasers synchronized by injection-locking and are blue-detuned from the trapping transition $^2S_{1/2}(F=3) \rightarrow ^2P_{3/2}(F'=4)$ by $\Delta = 2\pi \cdot 140$ MHz $\approx 23.3\Gamma$, where Γ denotes the natural linewidth. Such big detuning reduces the perturbation of atoms to a very low level (scattering rate $\propto 1/\Delta^2$) which is essential for non-destructive measurements. Moreover, non-resonant pump eliminates overlap of the RIRs and Raman-Zeeman resonances [6] hence facilitates interpretation of the results. Despite large Δ , the pump and probe beams drive the Raman signal with a sufficiently large amplitude and signal-to-noise ratio for the pump beam intensities 5–35 mW/cm².

The probe beam is scanned by $\delta \approx \pm 1$ MHz around frequency ω of the pump. The probe and pump photons induce Raman transitions between atomic kinetic states separated by $\pm \hbar\delta$. Since the polarization of the pump and probe beams is chosen to be the same, the atoms undergo Raman transitions with $\Delta m_F = 0$. Hence, the internal atomic state does not change and the only states that have to be considered are the external states associated with the kinetic energy of the atomic center-of-mass. The multi-level structure of ^{85}Rb can thus be reduced to a set of independent two-level systems which allows straightforward application of the basic RIR theory [1, 6, 7]. With the assumption that $\Pi(\mathbf{p})$ is the Maxwell-Boltzmann distribution, the RIR signal $s(\delta)$ [6, 7] recorded with the retroreflected probe is given by two contributions. The narrow one results from the Raman process involving the pump and the probe beam making small angle θ and the wide one is for angle $180^\circ - \theta$. The signal is

$$s(\delta) \propto -A_{\perp} \delta \exp\left(-\frac{\delta^2}{\xi_{\perp}^2}\right) - A_{\parallel} \delta \exp\left(-\frac{(\delta - \delta_0)^2}{\xi_{\parallel}^2}\right), \quad (1)$$

where, for small θ , $\xi_{\perp}^2 \approx 2k_B k^2 m^{-1} \theta^2 \tau_{\perp}$ and $\xi_{\parallel}^2 \approx$

$8k_B k^2 m^{-1} \tau_{\parallel}$. τ_{\perp} and τ_{\parallel} are the distribution widths in the \perp and \parallel directions in the temperature units, A_{\parallel} and A_{\perp} are the amplitudes of the corresponding contributions, m is the atomic mass, k_B is the Boltzmann constant, and δ_0 is the possible frequency shift between the \perp and \parallel contributions, to be discussed later.

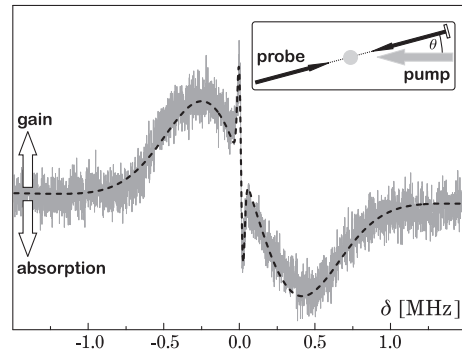


Figure 3: Transmission spectrum of a retroreflected probe (gray) and the theoretical prediction (dashed) of Eq.(1). Inset: the beam setup. The MOT beams have intensity $I_{\text{MOT}} = 13.8$ mW/cm² per beam and are detuned from the trapping transition by $\Delta_{\text{MOT}} = -3\Gamma$, the repumper beam intensity $I_{\text{REP}} = 15$ mW/cm², the axial magnetic field gradient $\partial_x B = 12$ Gauss/cm, the pump beam intensity $I = 33$ mW/cm², and the probe beam intensity 0.3 mW/cm².

Typical example of the retroreflected-probe transmission spectrum is shown in Fig. 3. It exhibits two distinct resonant contributions, predicted by eq. (1). The wide contribution is shifted with respect to the narrow one by 72.4 kHz, which indicates a 2.8-cm/s average velocity component in the \parallel direction. We thus observe an atomic drift within a cloud, which as a whole remains stationary. We understand this as a dynamic effect resulting from a small difference of the radiation pressures intrinsic to a MOT with retroreflected trapping beams. Indeed, the observed shift increases when the imbalance is purposely increased. Strong imbalance normally produces a displacement of the atomic-cloud center of mass. In our case this displacement is too weak to be detected by standard imaging technique, while the anisotropic atomic flow, even one order of magnitude slower than the mean thermal velocity, is well measurable with our method.

As the velocity distributions derived from the signal in Fig. 3 are Gaussian, one can determine the values $\tau_{\perp} = 172 \pm 6 \mu\text{K}$ and $\tau_{\parallel} = 170 \pm 3 \mu\text{K}$. The equality of these τ s implies thermodynamical equilibrium and allows their interpretation as temperature T , despite the slow drift. The equilibrium persists for various MOT-light intensities due to the fact that total intensities of each pair of the MOT beams remain the same. The observed nearly linear increase of T with the total MOT-beam intensity agrees well with previous reports [10, 11, 12].

The thermodynamics of the system becomes highly non-trivial when the trapping light is unevenly distributed between the MOT beam pairs. It was predicted that for such conditions the width of kinetic momentum

distribution shows directional dependence [13]. Using the simultaneous measurement of the momentum width in two perpendicular directions, we attempted to observe such anisotropic non-equilibrium state of the cold-atom cloud. For this reason, we changed intensity balance between the longitudinal (I_z) and transverse (I_x, I_y) MOT beam pairs, while keeping the total intensity $I_0 = I_x + I_y + I_z$ constant. We define parameter κ as the relative intensity of I_z , $I_z = \kappa I_0$, $I_x = I_y = (1 - \kappa)I_0/2$. The results of the measurement of τ_{\parallel} and τ_{\perp} for different values of κ are depicted in Fig 4. For equal partition of the trapping intensity ($\kappa = 1/3$), the widths of kinetic momentum distributions are the same, as expected. However, when κ increases, τ_{\parallel} and τ_{\perp} follow opposite trends, which is evidence of kinetic momentum anisotropy in a MOT working MOT and thereby its non-equilibrium state. A similar anisotropy was recently observed also in an optically dense sample [14]. We notice that $\tau_{\parallel} + 2\tau_{\perp}$, which is the measure of $v_{\parallel}^2 + 2v_{\perp}^2$, is constant within $\pm 2\%$ over the whole measured range of κ . The decrease of τ_{\parallel} with the growing κ is due to the fact that the heating associated with spontaneous emission is isotropic, whereas the cooling rate is higher for the direction with the increased intensity. The momentum anisotropy becomes manifest because the density of the atoms is too small to provide efficient thermalization. Indeed, simple estimation for typical conditions and Rb-Rb collision cross-section $\sigma_{\text{Rb-Rb}} = 3 \cdot 10^{-13} \text{ cm}^2$ [15] yields the atomic collision rate below 1 Hz in our trap, while the friction coefficient, in frequency units, is in the kHz range.

The theoretical behavior of τ_{\parallel} and τ_{\perp} according to Refs. [13, 16] is plotted in Fig. 4 along with the experimental data. They exhibit similar qualitative dependence (the decrease of τ_{\parallel} and the increase of τ_{\perp} with growing κ), but the existing theory fails to reproduce the exact shape of the experimental dependence. This discrepancy is due to additional mechanism of sub-Doppler cooling, not included in the calculations of Ref. [13]. Indeed, the increase of I_z accompanied by attenuation of I_x and I_y results in efficient quasi-1D cooling scheme in the $\sigma^+ - \sigma^-$ optical molasses [17]. Evidence of this cooling is provided by the values of τ_{\parallel} falling to $70 \mu\text{K}$, well below the Doppler cooling limit of $140 \mu\text{K}$. Importance of sub-Doppler cooling for anisotropy of momentum distribution in cold atomic samples has been previously noted in optical molasses [18].

In the situation discussed above, the MOT beams were carefully aligned which resulted in high stability of the trapped-atom cloud, even for the largest departures from the equal partition of the trapping light intensity, and allowed fitting of the RIR signals by eq. (1). The sole manifestation of the non-equilibrium of the sample was the $\Pi(p_{\perp})$ vs. $\Pi(p_{\parallel})$ anisotropy. The thermodynamical equilibrium can be altered yet in a different way, namely by enhancing imbalance between the counter-propagating MOT-beam radiation pressures. Fig. 5a depicts the RIR recorded with a standard 1D, two-beam

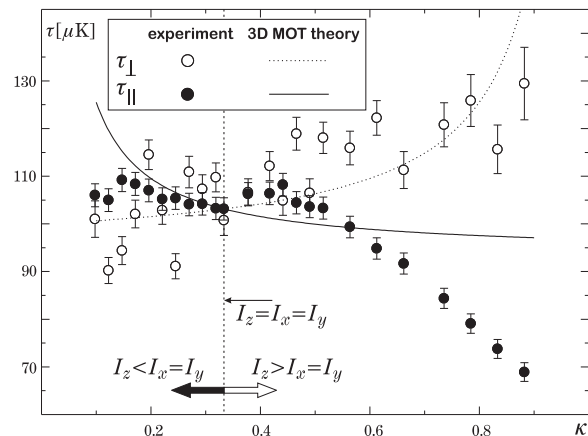


Figure 4: Widths of the kinetic momentum distributions measured as a function of relative intensity κ in the two perpendicular directions, τ_{\perp} (hollow circles) and τ_{\parallel} (filled circles). For the equilibrium ($\kappa = 1/3$), $I_{\text{MOT}} = 6.8 \text{ mW/cm}^2$, $\tau_{\perp} = 100 \pm 3 \mu\text{K}$, and $\tau_{\parallel} = 103 \pm 2 \mu\text{K}$. Other parameters as in Fig. 3. Theoretical curves are plotted according to Refs. [13, 16].

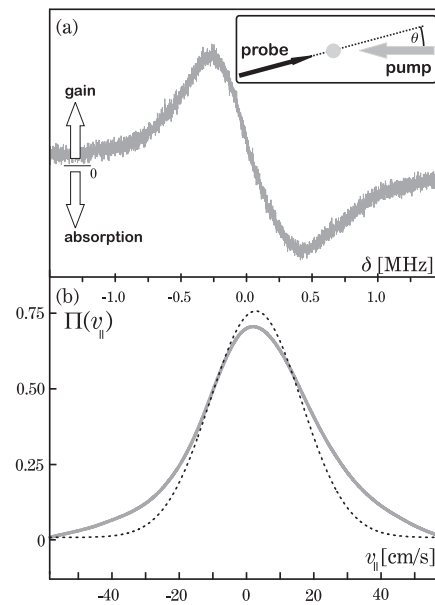


Figure 5: (a) The probe transmission spectrum in a misaligned MOT for $I_{\text{MOT}} = 3.1 \text{ mW/cm}^2$, $\Delta_{\text{MOT}} = -2.25\Gamma$ and other experimental parameters as in Fig 3. As shown in inset, the probe-beam is not retroreflected, hence only the wide RIR contribution is present. (b) The actual velocity distribution $\Pi(v_{\parallel})$ (grey thick line) obtained by integrating the probe transmission spectrum and the Gaussian reference (dotted line), defined in text.

arrangement applied to the case when the MOT beams were slightly misaligned and tuned closer to resonance. The 1D thermometry was accomplished by replacing the optional mirror in Fig. 2 by a photodiode. In this configuration, the pump and the probe make angle $180^\circ - \theta$ and

the recorded signal is proportional only to $\partial\Pi(p_{||})/\partial p_{||}$. Its shape deviates from a derivative of a Gaussian. By integrating the signal and scaling to the velocity units, the actual distribution of velocity component in the $||$ direction, $v_{||}$, can be retrieved. Fig. 5b shows such a distribution obtained from the experimental signal and the idealized Gaussian reference curve of the same area and of the width derived from the positions of the minimum and maximum of the RIR signal in Fig. 5a. Non-standard properties of a stable atomic gas, revealed in our experiment call for thorough theoretical analysis with proper accounting for cooling and heating mechanisms.

In conclusion, we have developed three-beam spectroscopic method of determining the momentum distributions of cold, trapped atoms, based on recoil-induced resonances. The method is non-destructive, highly sensitive and provides multi-dimensional momentum determination in a single measurement. Its potential has been demonstrated by study of three different momentum distributions of atoms in the operating magneto-optical trap: (i) thermodynamic equilibrium with well defined temperature and Gaussian momentum distribution with a slow velocity drift; (ii) non-equilibrium state characterized by Gaussian distributions with drastically different widths in the longitudinal and transverse directions; (iii) non-equilibrium state of non-Gaussian momentum

distribution along one direction. The result (ii) qualitatively confirms theoretical predictions of Ref. [13] and indicate need for more refined MOT theory. Our method can be particularly useful for studies of anisotropy in optical molasses [18], 2D MOTs [19], etc. The described method can be also straightforwardly applied to 3D case by introducing additional pump beam in the xz plane in Fig. 2. To avoid overlapping of the RIR signals associated with all $\Delta\mathbf{p}$ directions, the frequency of the additional pump could be shifted. Such an approach can be used for the non-destructive, on-line diagnostics of the atom dynamics in a trap carried out independently and simultaneously with other spectroscopic measurements. The method should also be applicable to quantum-degenerate gases. In fact, the widely used Bragg spectroscopy is based on the same principle of momentum and energy transfer. Measuring the Bragg-beam transmission in our three-beam geometry, rather than imaging BEC can thus become a valuable, non-destructive alternative.

This work was supported by the Polish Ministry of Science and Information Society Technologies and is part of a general program on cold-atom physics of the National Laboratory of AMO Physics in Toruń, Poland. Authors would like to thank Mariusz Gajda for his illuminating discussion and Krzysztof Sacha and Dmitry Budker for their valuable comments.

-
- [1] J.-Y. Courtois, G. Grynberg, B. Lounis, and P. Verkerk, *Phys. Rev. Lett.* **72**, 3017 (1994).
- [2] D.R. Meacher, D. Boiron, H. Metcalf, C. Salomon, and G. Grynberg, *Phys. Rev. A* **50**, R1992 (1994).
- [3] M.C. Fischer, A.M. Dudarev, B. Gutiérrez-Medina, and M.G. Raizen, *J. Opt. B: Quantum Semiclass. Opt.* **3**, 279 (2001).
- [4] G. Di Domenico, G. Miletì and P. Thomann, *Phys. Rev. A* **64**, 043408-1 (2001).
- [5] Y.-C. Chen, Y.-W. Chen, J.-J. Su, J.-Y. Huang, and I.A. Yu, *Phys. Rev. A* **63**, 043808 (2001).
- [6] T.M. Brzozowski, M. Brzozowska, J. Zachorowski, M. Zawada, and W. Gawlik, *Phys. Rev. A* **71**, 013401 (2005).
- [7] P. Verkerk, *Proceedings of The International School of Physics, Varenna, Course CXXXI*, 325 (1996).
- [8] J. Guo, P.R. Berman, B. Dubetsky, and G. Grynberg, *Phys. Rev. A* **46**, 1426 (1992); J. Guo and P.R. Berman, *ibid.* **47**, 4128 (1993); B. Dubetsky and P.R. Berman, *ibid.* **52**, R2519 (1995).
- [9] E.L. Raab, M. Prentiss, A. Cable, S. Chu, and D.E. Pritchard, *Phys. Rev. Lett.* **59**, 2631 (1987).
- [10] P.D. Lett, W.D. Phillips, S.L. Rolston, C.E. Tanner, R.N. Watts, C.I. Westbrook, *J. Opt. Soc. Am. B* **6**, 2085 (1989).
- [11] C.D. Wallace, T.P. Dinneen, K.Y.N. Tan, A. Kumarakrishnan, P.L. Gould and J. Javanainen, *J. Opt. Soc. Am. B*, **11**, 703 (1994).
- [12] X. Xu, T.H. Loftus, M.J. Smith, J.L. Hall and A. Gallagher and J. Ye, *Phys. Rev. A* **66**, 011401(R) (2002).
- [13] M. Gajda and J. Mostowski, *Phys. Rev. A* **49**, 4864 (1994).
- [14] A. Vorozcovs, M. Weel, S. Beattie, S. Cauchi, and A. Kumarakrishnan, *J. Opt. Soc. Am. B* **22**, 943 (2005).
- [15] U.D. Rapol and A. Wasan and V. Natarajan, *Phys. Rev. A*, **64**, 023402 (2001).
- [16] M. Gajda, *private communication*.
- [17] J. Dalibard and C. Cohen-Tannoudji, *J. Opt. Soc. Am. B* **6**, 2023 (1998).
- [18] J. Javanainen, *Phys. Rev. A* **46**, 5819 (1992), J. Javanainen, *J. Phys. B: At. Mol. Phys.* **27**, L41 (1994), Y. Castin and K. Mølmer, *Phys. Rev. Lett.* **74**, 3772 (1995).
- [19] K. Dieckmann, R.J.C. Spreeuw, M. Weidemüller, and J.T.M. Walraven, *Phys. Rev. A* **58**, 3891 (1998); J. Schoser, A. Batär, R. Löw, V. Schweikhard, A. Grabowski, Yu.B. Ovchinnikov, and T. Pfau *Phys. Rev. A* **66**, 023410 (2002); M. Vengalattore and M. Prentiss, *Phys. Rev. A* **72**, 021401(R) (2005).